ELSEVIER

Clinical Neurophysiology 111 (2000) 1974–1980

www.elsevier.com/locate/clinph

Acquiring simultaneous EEG and functional MRI☆

Robin I. Goldman[a,*], John M. Stern[b], Jerome Engel Jr[b], Mark S. Cohen[a]

[a]*UCLA Brain Mapping Division, Ahmanson-Lovelace Brain Mapping Center, 660 Charles E. Young Drive South, Los Angeles, CA 90095-7085, USA*
[b]*Department of Neurology, Reed Neurological Research Center, UCLA School of Medicine, Los Angeles, CA 90095-1769, USA*

Accepted 28 August 2000

Abstract

Objective: Electroencephalography (EEG) is a challenge to record simultaneously with functional MRI (fMRI), for it is prone to large artifacts induced by both the static and the time-variant fields of the MR scanner. However, truly concurrent EEG/fMRI recording has great potential for clinical and scientific neurological applications. We have devised a method for acquiring EEG simultaneously with fMRI that minimizes contamination of the EEG signals.

Methods: We recorded EEG differentially during fMRI using special twisted dual-lead electrodes in a bipolar montage, and a combination of analog pre-processing and digital post-processing of the EEG data. We implemented a functional scan protocol that typically yields artifact-free EEG over 87% of the MR scanning period.

Results: Our approach greatly reduced gradient, radio frequency, motion and ballistocardiographic artifact in the EEG, and allowed continuous monitoring of the EEG during functional scanning. To illustrate the quality of the EEG following post-processing, we demonstrated that EEG recorded during fMRI retains useful spectral information.

Conclusions: Quality EEG may be recorded simultaneously with fMRI. With this union, activation maps could be made of any relevant changes in the EEG, such as inter-ictal spikes or spectral variations, or of evoked response potentials (ERPs).

Keywords: Electroencephalography; Functional MRI; Artifact; Brain mapping; Localization, Evoked response potential

1. Introduction

Electroencephalography (EEG) has been a key tool in the study of the brain for decades (Caton, 1875; Berger, 1929). However, despite its multiple clinical and research uses, such as in epilepsy (Ebersole, 1997), sleep staging (Rechtschaffen and Kales, 1968) and psychophysiology (Jewett et al., 1970; Hoptman and Davidson 1998; Pizzagalli et al., 1999), little is yet known about the underlying generators of EEG activity in humans (Elul, 1972). Functional MRI (fMRI) recorded in concert with EEG may provide a method for localizing and identifying these sources. By using the EEG signal as a reference for fMRI maps, concurrent EEG/fMRI opens a new avenue for investigating specific brain function. Toward this end, we set out to design a system for simultaneous recording of EEG and fMRI.

Concurrent acquisition of EEG and fMRI has proven challenging. Time varying magnetic (B) fields induce an electromotive force (EMF) in a wire loop perpendicular to the B field direction which, by Lenz's Law, is proportional to the cross sectional area of the wire loop and to the rate of change of the perpendicular magnetic field (dB/dt). When EEG leads are placed inside the MR scanner, the rapidly changing gradient fields and the radio-frequency (rf) pulses required for MRI may induce voltages that obscure the EEG signal (Ives et al., 1993; Huang-Hellinger et al., 1995). This induced EMF yields currents that can heat the electrodes and leads and potentially impart burns to the patient (Lemieux et al., 1997). Motion of the leads themselves within the static field of the magnet also induces an EMF (Hill et al., 1995) – even pulsatile motion related to heart beat yields ballistocardiographic artifact in the EEG that can be of roughly the same magnitude as the EEG signals themselves (Ives et al., 1993; Muri et al., 1998; Goldman et al., 2000). Further, introduction of EEG equipment into the scanner potentially can disturb the homogeneity of the

☆ Portions of this material were presented previously at the 8th Scientific Meeting of the International Society for Magnetic Resonance in Medicine, Denver, CO, USA, April 2000, and at the 6th Annual Meeting of the Organization for Human Brain Mapping, San Antonio, TX, USA, June 2000.

* Corresponding author. Tel.: + 1-310-206-4456; fax: +1-310-794-7406.

E-mail address: rig@ucla.edu (R.I. Goldman).

1388-2457/00/$ - see front matter
CLINPH 2000098
PII: S1388-2457(00)00456-9

magnetic field and distort the resulting MR images (Ives et al., 1993).

In addition to the large artifacts in the EEG caused by high frequency gradient and rf pulses, the high pass filters of most EEG equipment lead to long signal recovery times once the MR sequence has terminated (Huang-Hellinger et al., 1995; Bonmassar et al., 1999; Krakow et al., 1999; Lovblad et al., 1999). One method used to overcome these difficulties in epilepsy studies has been to monitor the EEG in the absence of scanning while the patient is in the magnet and then trigger functional scanning manually after identification of inter-ictal spikes in the EEG record (Ives, 1995; Warach et al., 1996; Seeck et al., 1998; Krakow et al., 1999; Patel et al., 1999; Symms et al., 1999). This method takes advantage of the 3–5 s lag in BOLD response to obtain images of an event which occurred just prior to initiation of the scan. Others have used interleaved EEG and fMRI methods to study visual evoked potential, where the same stimuli are presented in each block (Bonmassar et al., 1999), and sleep (Huang-Hellinger et al., 1995; Lovblad et al., 1999).

In both the triggered and interleaved methods, EEG and fMRI are acquired serially, resulting in protocol limitations and problems with data analysis. In the triggered method, relevant changes in the EEG, such as subsequent spike activity, can not be seen during functional scanning. Also problematic is the non-uniform MR image contrast – T1 saturation typically does not reach equilibrium until 3–4 TRs after initiation of the scan (depending on TR and effective flip angle), but it is these first TRs that capture the BOLD response. In the interleaved method, in addition to the former confounds, data for each modality is acquired using stimuli displaced in time, and thus, the EEG can not be used as a direct reference function for fMRI signal maps.

We have developed a method for acquiring simultaneous EEG and fMRI that utilizes a combination of analog preprocessing and digital post-processing to strongly suppress the common artifacts. With this method, we have been able to implement a functional scan protocol that yields windows of artifact-free EEG between short gradient and rf bursts and allows continuous monitoring of the EEG during functional scanning. Although not the central focus of this report, we note that the technologies we have described here are applicable equally to evoked response potentials (ERPs) which differ from EEG studies in interpretation more than in technique.

2. Methods

2.1. EEG device and lead placement

Our EEG device incorporates numerous hardware modifications to reduce artifact in concurrent EEG/fMRI. It was built by Telefactor Corporation (W. Conshohocken, PA) in collaboration with our team, and was modified specifically for our application. We detected signal from the scalp using silver chloride plated plastic cup electrodes connected to a compact magnet-compatible local amplifier (headbox) via 10 foot carbon fiber leads with a resistance of 1 kΩ/foot. This design minimized both artifact in the MR images and the induction of rf current loops in the lead wires.

We devised a lead configuration that minimized unwanted current induction by recording EEG in a hard-

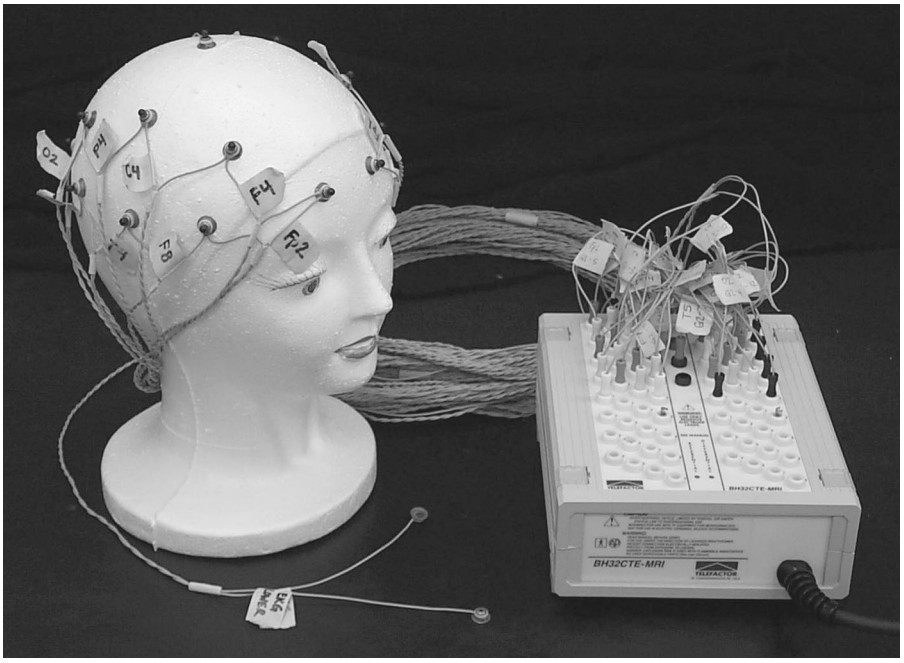

Fig. 1. Chained bipolar dual-lead dress. Leads of consecutive electrodes are twisted together to reduce scanner artifact.

wired montage using special dual-lead electrodes. We twisted the lead wires from each electrode pair together for their entire length, forming a chained bipolar montage for each hemisphere (Fp2-F8, F8-T4, T4-T6, T6-O2, O2-P4, P4-C4, C4-F4, F4-Fp2; Fpl-F7, F7-T3, T3-T5, T5-O1, O1-P3, P3-C3, C3-F3, F3-Fp1). The dual leads allowed each differential pair to be twisted together (Figs. 1 and 2A); the resulting configuration leaves only small loops at the head in which current can be induced. As shown in Fig. 2B, currents induced by motion and gradient switching will be self-canceling, for the current induced in consecutive twists will flow in opposing directions in each lead wire.

The magnet-compatible headbox contains 32 separate channel inputs, each with a differential amplifier coupled to a low pass RC filter with a time constant of 0.25 ms. This low pass filter attenuates the large waveforms induced by the rapidly changing magnetic fields of the scanner and yields very rapid recovery of the EEG signal following MR slice acquisition. We used 16 channels to record EEG, and two additional channels for electrocardiogram (EKG) and a scan trigger (see below). The EKG was acquired using a pair of twisted single-lead electrodes placed above and below the heart on the subject's back. This placement minimized lead motion, and thus electrical artifact, due to breathing. We used a scan trigger channel to receive a pulse from the scanner every TR to aid in post-processing of the data, and filtered the signal in all channels with a band pass of 0.5–70 Hz to further attenuate high frequency noise.

We fed the signal to a battery powered isocoder containing an A/D converter where it was sampled at 200 Hz, and the digitized signal was carried out of the shielded magnet room via optical fiber to maintain the scanner's electromagnetic isolation. After translation to Transistor-Transistor Logic (TTL), we routed the data to a Telefactor Digital EEG (D/EEG). We could then view the EEG data in real time and send it off-line via a 10baseT Ethernet connection to a post-processing and viewing station for further artifact attenuation.

2.2. Scan protocol

All subjects signed a consent form approved by the UCLA Human Subject Protection Committee prior to MR scanning, which we performed in our General Electric (Waukesha, WI) 3T scanner modified for echo planar imaging (EPI) by Advanced NMR Systems. We provided no visual or auditory stimulation for the subjects during functional scanning.

We first acquired scout scans of the entire brain to localize slice planes parallel to the ACPC line through the occipital cortex. To acquire EEG during functional scanning, we then prescribed a scan protocol which allowed windows of readable EEG between gradient bursts. We used an EPI sequence with TR = 4000 ms, TE = 45 ms, 64×64 matrix, 20×20 cm FOV, 4 mm slice thickness, and 1 mm gap to collect 6 slices spaced evenly over the TR period, leaving a 580 ms window of readable EEG between each 90 ms period of gradient induced noise (an 87% duty cycle).

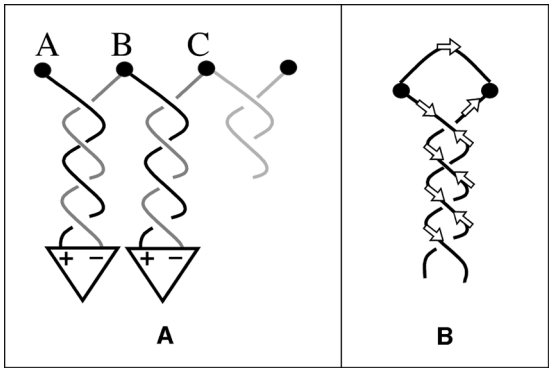

Fig. 2. (A) Dual-lead electrodes allow each bipolar pair to be twisted together for their entire length, sending signal directly to the local differential amplifiers. (B) Twisting leaves only small loops at the head in which EMF can be induced, for current (arrows) induced in lead twists by motion and gradient switching will be self canceling.

2.3. Artifact reduction post processing

We performed post-processing and viewing on a Dell Inspiron 3000 Pentium PC. After importing data from the D/EEG, we viewed the EEG data with Telefactor Twin software (version 1.50), and processed it further using home-built software described below to remove remaining artifacts. The residual artifact included both noise from EMF induced by the magnetic field gradients (which appeared in the EEG when a slice was acquired) and ballistocardiogram. The latter occurred in the EEG in a fairly regular pattern following each heart contraction, but its morphology and amplitude differed in each EEG channel.

To suppress gradient artifact in the EEG record, we utilized a 5 μs trigger pulse generated by the scanner each TR. Because the EEG was digitized at 200 Hz, we conditioned this pulse by broadening it to 50 ms using a simple monostable multivibrator circuit (schematic available upon request). In post-processing, we then used this scan trigger to initiate a blanking scheme. Following each trigger, we replaced 90 ms of digital data in the EEG and EKG with zeros every time $t = \mathrm{TR}/n$, where n = number of slices. This way, the electrical record was zeroed during each slice acquisition.

Next, we averaged together sections of EEG following a cardiac trigger to yield the ballistocardiographic artifact. In order to identify the initiation of each cardiac pulse, we used a single artifact-free QRS wave segment of the subject's EKG, recorded inside the scanner when no scanning was taking place, as a reference (see Fig. 3A). We compared this reference wave segment to portions of the EKG data of the same length, shifted by one data point at a time, and calculated a correlation coefficient (CC) for each corresponding data portion. When the CC exceeded an empirically selected value (typically 0.7), we identified the peak CC following

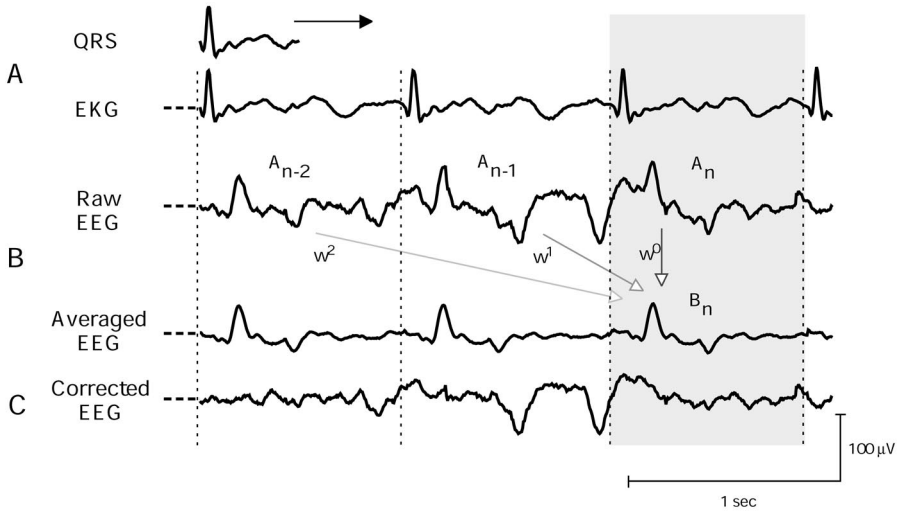

Fig. 3. The ballistocardiogram subtraction algorithm, shown using data collected on a normal volunteer. EKG was scaled down by a factor of 15 for this figure. (A) We correlated a segment of the subject's QRS wave to their EKG, and peak correlation values initiated a trigger (shown by the vertical dotted lines). (B) We then averaged together trigger to trigger segments, weighting segments less and less by temporal displacement from the *n*th (shaded) segment. (C) We subtracted the averaged data from the raw EEG to yield ballistocardiogram-free EEG.

this threshold crossing to trigger the initiation of ballistocardiogram averaging and subtraction.

Fig. 3B illustrates the averaging and subtraction algorithm we performed on the data in each EEG channel. We averaged every trigger-to-trigger section of raw EEG data (A_n) with all preceding sections. Because EEG and EKG should be uncorrelated, this method averaged out the EEG signal and left only ballistocardiogram (B_n). We weighted data sections inversely with their temporal displacement from the current sample to compensate for slow changes in the ballistocardiographic artifact, calculating the ballistocardiogram in each trigger to trigger section using the weighted average

$$B_n = \frac{\sum_{i=0}^{n} w^i A_{n-1}}{\sum_{i=0}^{n} w^i}$$

with a weighting factor $w = 0.9$. Thus, the earlier cycles formed an exponentially decreasing contribution with a time constant of roughly 10 sections. We then subtracted the averaged wave, B_n, calculated separately for each channel, from that channel's raw EEG, A_n, to yield artifact-free corrected EEG (Fig. 3C).

We accounted for variations in section length due to changes in heart rate by averaging sections point-by-point. The first data point in each section was averaged with the first data point in previous sections, the second with the second, etc. Data points at the end of longer sections were averaged with corresponding points in other long sections, and the weighting factors of each point were adjusted accordingly. To avoid subtracting data with too few points averaged, we performed the subtraction only if 3 or more points were used in the calculation; otherwise, the raw data remained in the final record.

Our method of ballistocardiogram removal is conceptually similar to that of Allen et al. (1998) but differs in the weighting applied to earlier EEG data, and therefore in its sensitivity to drift.

2.4. Characterization of noise reduction: phantom study

To characterize noise reduction due to our twisted dual-lead dress, we performed scanning experiments using a biological phantom – a 7 pound human head-sized grocery store roasting chicken – and compared twisted vs. untwisted lead arrangements. We placed the leads at distances corresponding approximately to standard international 10–20 positions on the phantom. On the left hemisphere, we placed the 8 electrode chained twisted montage detailed above, and on the right we placed a matching dual-lead non-twisted montage. A scout scan was acquired to position the functional slices to cover the phantom. We then performed functional EPI scans as described previously.

We analyzed the EEG data to quantify noise reduction due to the lead dress, calculating the loss, in dB, using 30 s data segments as

$$\mathrm{dB} = 20\log \frac{\overline{\sqrt{\sum V_{\mathrm{twist}}^2}}}{\sqrt{\sum V_{\mathrm{no-twist}}^2}}$$

where we summed data points over each channel separately, then averaged over all twisted and all untwisted channels. We calculated gradient noise reduction due to lead twisting by subtracting the square root of the sum of the squared voltages without scanning from that during scanning for

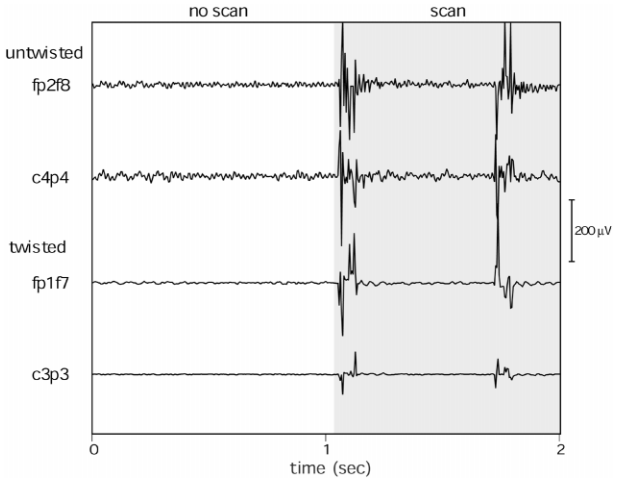

Fig. 4. EEG of a non-living biological phantom recorded inside the MR scanner using twisted and untwisted leads, showing recordings both in absence of scanning and during EPI. Note that all signal in these traces is caused by either field variance in the MRI or other non-physiological sources (vibration, radio waves in the scan room, etc.). With or without scanning, EEG recorded using the untwisted leads was significantly noisier.

both twisted and untwisted lead data, and then calculated attenuation as above.

2.5. Characterization of noise reduction: human study

To characterize twisted lead noise reduction further, we repeated the above study on a 23-year-old normal male volunteer. Again, the chained twisted lead set was placed on the subject's left hemisphere, and the untwisted set on the subject's right. We recorded his EEG inside the MR scanner, both with and without scanning. We then calculated noise reduction as the power loss (in dB) for twisted vs. untwisted leads, both before and after post-processing. We also estimated the power of the artifact in each lead set as the reduction in dB after vs. before post-processing.

2.6. Spectral analysis

By restricting the timing of the EPI acquisitions to fall outside of the frequency band of interest for EEG (e.g., to study alpha activity, the scanning rate should be less than 4 images/s), we were able to retain useful EEG spectral information. (We have not yet evaluated the magnitude of the contamination that might occur at different TRs.) To illustrate this, we scanned a 28 year-old normal female volunteer during a standard eyes open, eyes closed task known to activate alpha rhythm. We instructed the subject to open and then close her eyes at 30 s intervals for the 3 min 30 s functional scan (TR = 2500 ms, TE = 45 ms, 64×64 matrix, 20×20 cm FOV, 4 mm slice thickness, and 1 mm gap to collect 4 slices centered on occipital cortex). After post-processing the EEG to remove artifact, we calculated the alpha power in each TR using software developed in-house. With this software, we calculated the EEG power vs. spectral frequency with each TR using the fast Fourier transform.

3. Results

3.1. Noise reduction due to lead dress: phantom study

EEG recorded on the phantom using the untwisted leads was substantially noisier than that recorded using their twisted counterparts. Fig. 4 shows the recorded EEG in both twisted and untwisted lead channels. When not scanning, the twisted leads reduced random noise power by an average of 5.4 dB. During scanning, gradients caused large artifacts in both the twisted and untwisted lead sets, but this noise power was reduced by an average of 6.3 dB in the twisted leads.

3.2. Twisted vs. untwisted leads on a volunteer

Fig. 5A shows the raw EEG data we recorded on a normal volunteer inside the scanner just before and just after initia-

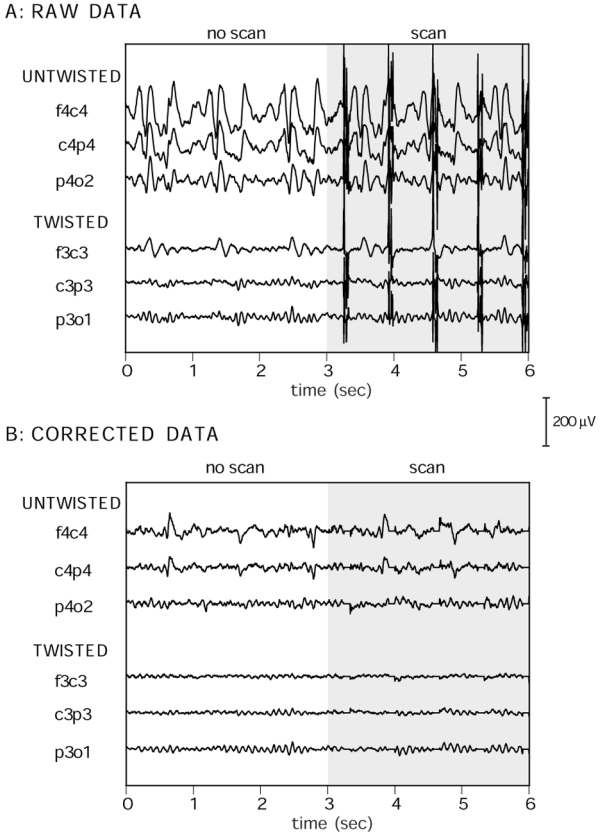

Fig. 5. (A) Raw BEG recorded inside the MR scanner before and after initiation of EPI, using untwisted leads on the normal volunteer's right hemisphere (shown at top) and twisted leads on the left hemisphere (bottom). BEG recorded with the untwisted leads was significantly noisier. Ballistocardiogram is visible in the twisted lead data, but is reduced compared to the untwisted. (B) The same data shown in (A), following artifact reduction post-processing. The untwisted lead data still contains significant artifact.

tion of the EPI sequence in 3 representative twisted and three comparable untwisted channels. EEG recorded with the untwisted leads was significantly noisier, and while ballistocardiogram was visible in the twisted lead data, it was reduced compared to the data recorded with the untwisted leads. Twisting the leads reduced overall noise by an average of 9.4 dB across all channels when not scanning. In preliminary studies, reduction was found to vary from 0.4 to 7.5 dB. During EPI, twisting reduced noise by 5.5 dB.

3.3. Noise reduction due to artifact post-processing

The same data in Fig. 5A is presented after post-processing in Fig. 5B. The post-processing removed significant gradient and rf artifact, as well as ballistocardiogram. Post-processing of the data recorded before initiation of scanning removed 6.5 dB in the twisted leads and 10.2 dB in the untwisted leads, largely because the ballistocardiogam was greater in the data from the untwisted leads. In data recorded during scanning, post-processing removed 15.3 dB in the twisted leads and 15.0 dB in the untwisted. Importantly, post-processing produced similar noise reduction in twisted vs. untwisted leads in data both before (5.7 dB) and during EPI (5.8 dB).

3.4. Spectral analysis

When the subject's eyes were closed, power in the alpha band, between 8 and 12 Hz, increased greatly (Fig. 6). And as is expected, this alpha signal was not present when the subject's eyes were open.

4. Discussion

Using a combination of analog pre-processing and digital post-processing, we can acquire artifact-free EEG recorded simultaneously with functional MRI. While the EEG is obscured during gradient bursts, it recovers quickly and therefore no significant data loss occurs between slice acquisitions. Further, because we digitally blank the data record for the duration of MR gradient bursts, the gradient-induced deflections do not corrupt the EEG record in the post-processing averaging algorithm we use to remove ballistocardiogram. Although with our method a trade off must be made between brain coverage in functional scanning and the fraction of useable EEG in the data record, a long TR allows acquisition of a reasonable number of slices. And, if the timing of slice acquisition does not overlap with desired spectral frequencies, the spectral power can be calculated in EEG recorded during functional mapping.

Because we are able to acquire EEG continuously through functional scanning, we do not encounter the problems of initially non-uniform MR image contrast inherent in interleaved EEG/fMRI methods. Most often this contrast non-uniformity has been handled by ignoring images acquired in the first 3–4 TRs, but this leads to an inherent time delay in the functional scanning. While this could be mitigated to some degree by using schemes that correct for the T1-related intensity differences based on the actual TR (Guimaraes et al., 1998; DuBois and Cohen, 2000), methods which avoid this dilemma are preferable.

We have therefore developed a potentially powerful method for localizing the sources of various EEG wave forms. Because the EEG is acquired simultaneously rather that serially with fMRI, it can be used as a direct source for the fMRI reference function. In this way, activation maps could be made of any relevant variations in the EEG, such as spike and slow wave patterns in epilepsy, or spectral changes. This feature of truly simultaneous electrical recording and magnetic imaging may be of particular value in ERP studies combined with fMRI.

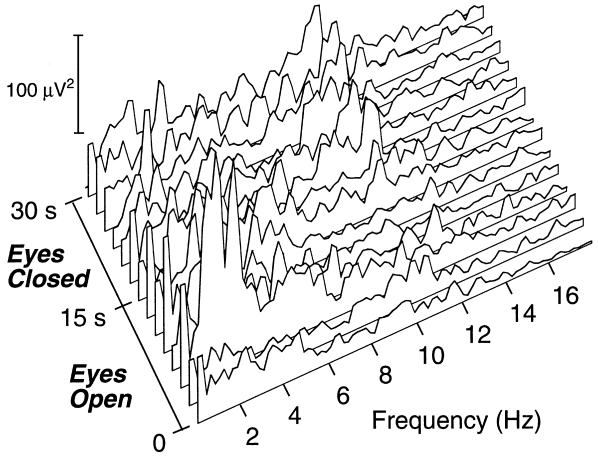

Fig. 6. Power spectrum of EEG (p3o1) recorded simultaneously with fMRI, in steps equal to the TR of 2.5 s, showing expected increases in the alpha band (8–12 Hz) when the subject's eyes were closed.

Acknowledgements

This work was supported in part by grant number R01-DA13054-01 from the National Institute on Drug Abuse. R.I.G. was supported by a Eugene Cota-Robles Fellowship from UCLA. We wish to acknowledge the generous support of the Brain Mapping Medical Research Foundation, The Ahmanson Foundation, the Pierson-Lovelace Foundation, the Jennifer Jones Simon Foundation, the Tamkin Foundation, the UCLA Council on Research, and the Grass-Telefactor Division of Astro-Med, Inc.

References

Allen PJ, Polizzi G, Krakow K, Fish DR, Lemieux L. Identification of EEG events in the MR scanner: the problem of pulse artifact and a method for its subtraction. Neuroimage 1998;8:229–239.

Berger H. Uber das elektrenkephalogramm des menschen. Archiv für Psychiatrie und Nervenkrankheiten 1929;87:527–570.

Bonmassar G, Anami K, Ives J, Belliveau JW. Visual evoked potential

(VEP) measured by simultaneous 64-channel BEG and 3T fMRI. NeuroReport 1999;10:1893–1897.

Caton R. The electric currents of the brain. Br Med J 1875;2:278.

DuBois RM, Cohen MS. Spatiotopic organization in human superior colliculus observed with fMRI. NeuroImage 2000 in press.

Ebersole JS. Defining epileptogenic foci: past, present, future. J Clin Neurophysiol 1997;14:470–483.

Elul R. The genesis of the EEG. Int Rev Neurobiol 1972;15:227–272.

Goldman RI, Cohen MS, Stern JM, Engel J, Combining EEG, functional MRI:. cleaning up the electrical signals. Proc Int Soc Mag Res Med 2000;8:19.

Guimaraes AR, Melcher JR, Talavage TM, Baker JR, Ledden P, Rosen BR, Kiang NY, Fullerton BC, Weisskoff RM. Imaging subcortical auditory activity in humans. Hum Brain Mapp 1998;6:33–41.

Hill RA, Chiappa KH, Huang-Hellinger F, Jenkins BG. EEG during MR imaging: differentiation of movement artifact from paroxysmal cortical activity. Neurology 1995;45:1942–1943.

Hoptman MJ, Davidson RJ. Baseline EEG asymmetries and performance on neuropsychological tasks. Neuropsychologia 1998;36:1343–1353.

Huang-Hellinger FR, Breiter HC, McCormack G, Cohen MS, Kwong KK, Sutton JP, Savoy RL, Weisskoff RM, Davis TL, Baker JR, Belliveau JW, Rosen BR. Simultaneous functional magnetic resonance imaging and electrophysiological recording. Hum Brain Mapp 1995;3:13–25.

Ives JR. Apparatus and method for recording an electroencephalogram during magnetic resonance imaging. USA. August 29, 1995. Patent No: 5,445,162

Ives JR, Warach S, Schmitt F, Edelman RR, Schomer DL. Monitoring the patient's EEG during echo planar MRI. Electroenceph clin Neurophysiol 1993;87:417–420.

Jewett DL, Romano MN, Williston JS. Human auditory evoked potentials: possible brain stem components detected on the scalp. Science 1970;167:1517–1518.

Krakow K, Woermann FG, Symms MR, Allen PJ, Lemieux L, Barker GJ, Duncan JS, Fish DR. EEG-triggered functional MRI of interictal epileptiform activity in patients with partial seizures. Brain 1999;122:1679–1688.

Lemieux L, Allen PJ, Franconi F, Symms MR, Fish DR. Recording of BEG during fMRI experiments: patient safety. Magn Reson Med 1997;38:943–952.

Lovblad KO, Thomas R, Jakob PM, Scammell T, Bassetti C, Griswold M, Ives J, Matheson J, Edelman RR, Warach S. Silent functional magnetic resonance imaging demonstrates focal activation in rapid eye movement sleep. Neurology 1999;53:2193–2195.

Muri RM, Felblinger J, Rosler KM, Jung B, Hess CW, Boesch C. Recording of electrical brain activity in a magnetic resonance environment: distorting effects of the static magnetic field. Magn Reson Med 1998;39:18–22.

Patel MR, Blum A, Pearlman JD, Yousuf N, Ives JR, Saeteng S, Schomer DL, Edelman RR. Echo-planar functional MR imaging of epilepsy with concurrent EEG monitoring. Am J Neuroradiol 1999;20:1916–1919.

Pizzagalli D, Regard M, Lehmann D. Rapid emotional face processing in the human right and left brain hemispheres: an ERP study. NeuroReport 1999;10:2691–2698.

Rechtschaffen A, Kales AA. A manual of standardized terminology, techniques, and scoring system for sleep stages of human subjects, Washington, DC: Public Health Service, 1968.

Seeck M, Lazeyras F, Michel CM, Blanke O, Gericke CA, Ives J, Delavelle J, Golay X, Haenggeli CA, deTribolet N, Landis T. Non-invasive epileptic focus localization using EEG-triggered functional MRI and electromagnetic tomography. Electroenceph clin Neurophysiol 1998;106:508–512.

Symms MR, Allen PJ, Woermann FG, Polizzi G, Krakow K, Barker GJ, Fish DR, Duncan JS. Reproducible localization of interictal epileptiform discharges using EEG-triggered fMRI. Phys Med Biol 1999;44:N161–N168.

Warach S, Ives JR, Schlaug G, Patel MR, Darby DG, Thangaraj V, Bdelman RR, Schomer DL. EEG-triggered echo-planar functional MRI in epilepsy. Neurology 1996;47:89–93.